Biophysical Journal
Article

Biophysical Society

Tropomyosins Regulate the Severing Activity of Gelsolin in Isoform-Dependent and Independent Manners

Nikolett Kis-Bicskei,[1] Bálint Bécsi,[2,3] Ferenc Erdődi,[2,3] Robert C. Robinson,[4,5] Beáta Bugyi,[1,6] Tamás Huber,[1] Miklós Nyitrai,[1,7,*] and Gábor Csaba Talián[1]

[1]Department of Biophysics, Medical School, University of Pécs, Pécs, Hungary; [2]Department of Medical Chemistry and [3]MTA-DE Cell Biology and Signaling Research Group, University of Debrecen, Faculty of Medicine, Debrecen, Hungary; [4]Institute of Molecular and Cell Biology, Agency for Science, Technology and Research, Singapore, Singapore; [5]Research Institute for Interdisciplinary Science, Okayama University, Okayama, Japan; [6]Szentágothai Research Center, University of Pécs, Pécs, Hungary; and [7]MTA-PTE Nuclear-Mitochondrial Interactions Research Group, Pécs, Hungary

ABSTRACT The actin cytoskeleton fulfills numerous key cellular functions, which are tightly regulated in activity, localization, and temporal patterning by actin binding proteins. Tropomyosins and gelsolin are two such filament-regulating proteins. Here, we investigate how the effects of tropomyosins are coupled to the binding and activity of gelsolin. We show that the three investigated tropomyosin isoforms (Tpm1.1, Tpm1.12, and Tpm3.1) bind to gelsolin with micromolar or submicromolar affinities. Tropomyosin binding enhances the activity of gelsolin in actin polymerization and depolymerization assays. However, the effects of the three tropomyosin isoforms varied. The tropomyosin isoforms studied also differed in their ability to protect pre-existing actin filaments from severing by gelsolin. Based on the observed specificity of the interactions between tropomyosins, actin filaments, and gelsolin, we propose that tropomyosin isoforms specify which populations of actin filaments should be targeted by, or protected from, gelsolin-mediated depolymerization in living cells.

INTRODUCTION

The actin cytoskeleton is a filamentous protein scaffold and a polymerizing motor underlying a plethora of essential cellular processes. These include cell motility, cytokinesis, endocytosis, contractility, and determination of cell shape and size. Most actin filaments are highly dynamic structures that participate in particular intracellular subsystems with distinct protein compositions and functions (1). These structures are governed by a large number of diverse actin-binding proteins (ABPs) that regulate the kinetics of events between filament ends and monomeric actin, establish the supramolecular organization of the microfilament system, and influence the binding of other protein partners to filaments.

In animal and fungal cells, most microfilaments are decorated with tropomyosins (Tpm) that, in addition to conferring actin isoform diversity, substantially contribute to the formation of the individual filament subcompartments (2,3). In mammals, four Tpm genes were demonstrated to produce >40 mRNA variants and ~25 isoforms at the protein level (4,5). Tropomyosins are always present as polar coiled-coil dimers that cooperatively polymerize in a head-to-tail manner and bind along the groove of the actin filament (6). Although the expression and localization of Tpm isoforms are strictly regulated according to cell type, developmental state, and pathologic condition (7), the origin and function of their diversity is not well understood. In rat neurons, the localization patterns of Tpm3.1/Tpm3.2 (formerly TM5NM1/TM5NM2) and Tpm1.12 (formerly TMBr-3) isoforms coded for by the *Tpm3* and *Tpm1* genes, respectively, undergo an isoform switch in the axon, which has been confirmed in chicken neurons (8). In early embryos and at the end of the first week of culture of primary cortical neurons, *Tpm3.1/Tpm3.2* mRNA and protein are present at the differentiating axonal pole, then, a few days later, principally relocalize to the developing axons (9). Around the 16th embryonic day, *Tpm3.1/Tpm3.2* mRNA is lost from the axons and the protein repositions into the somatodendritic compartment. This change of localization is accompanied by the continuous appearance of the Tpm1.12 isoform in the axons, where it resides in the mature neurons (8). In the growth cone of the developing nerve cells, the presence

Submitted July 12, 2017, and accepted for publication November 29, 2017.

*Correspondence: miklos.nyitrai@aok.pte.hu

Editor: Enrique De La Cruz.

https://doi.org/10.1016/j.bpj.2017.11.3812

of only Tpm3.1, and not Tpm1.12, has been demonstrated (10,11). These differences in the developmental profiles of the two Tpm isoforms are also reflected by their diverse cellular effects upon overexpression (12). In a B35 neuroepithelial cell line, Tpm1.12 reduced the cell size and the number of stress fibers, but promoted lamellipodium formation and cell motility. Tpm3.1 overexpression yielded contrasting impacts and enhanced the phosphorylation of the myosin II regulatory light chain and recruited the myosin IIA heavy chain to stress fibers, thus increasing contractility. Exogenous Tpm3.1 expression was accompanied by a higher extent of actin-depolymerizing factor (ADF) phosphorylation and desorption of ADF from the stabilized stress fibers. These findings demonstrate that the properties of the Tpm isoform that binds to the actin filament can be a deciding factor in the manifested molecular composition and cellular function.

Gelsolin belongs to a superfamily of structurally related ABPs (13). These proteins share common building blocks, the gelsolin-homology domains (14). Gelsolin was discovered as a factor inhibiting the sol-gel transition of the cortical actin cytoskeleton in macrophages (15). In the cytoplasm, gelsolin generally exists as a single isoform. In vitro, gelsolin is able to both nucleate and sever actin filaments, and it also caps the actin-filament barbed ends (16–18). These activities require the binding of Ca^{2+} to several conserved sites of the protein characterized by different affinities (13). Calcium binding unlatches the compact globular structure of gelsolin (19), allowing it to extend into a conformation with active binding sites for G-actin and F-actin on gelsolin-homology domains 1, 4, and 2–3 (19–21).

Tropomyosins have been shown to inhibit the ability of gelsolin to disassemble actin filaments (22). High-molecular-weight Tpms from fibroblasts and skeletal muscle when bound to F-actin prevented gelsolin from severing the actin filaments. The effect of the short Tpm isoforms was weaker but was potentiated by addition of caldesmon (22). It was shown that skeletal Tpm (Tpm1.1; in this article referred to as skeletal muscle Tpm (skTM)) promoted desorption of gelsolin from its complexes with β-actin and its sedimentation with actin filaments. Quantitative data suggested that upon formation of the Tpm-actin complexes, actin filaments undergo a conformational change that increases the dissociation of gelsolin (23). Skeletal Tpm can be chemically linked to gelsolin or retained on a gelsolin column in the presence of Ca^{2+}, which suggests a direct binding between the two proteins (24). This link was corroborated by the effect of skeletal and smooth muscle Tpms in protecting gelsolin from specific proteolytic cleavage by thermolysin (25). In this latter study, skeletal and smooth muscle Tpms were only able to protect actin filaments from severing when pre-incubated with gelsolin, but not when directly associated to actin filaments. A model was proposed in which free Tpm forms a complex with gelsolin, which passively removes it from the available pool (25).

To further extend the investigations of Tpm isoforms on the activities of gelsolin, in this study, we carried out experiments addressing the combined effects of gelsolin and Tpms on the polymerization properties of actin. Here, we found that the three investigated Tpms (skTM, Tpm1.12, and Tpm3.1) bind tightly to gelsolin. We show that the activity of gelsolin is enhanced in complexes with Tpms, resulting in higher polymerization and depolymerization rates, and that binding of Tpms to actin filaments prevented the depolymerizing activity of gelsolin to different extents depending on the Tpm isoform. We found that skeletal Tpm displayed a strong protective effect against severing by gelsolin. The other two Tpm isoforms did not show a significant effect. These interactions between actin and gelsolin specified by Tpm isoform lead to a simple model where Tpm isoforms can selectively mark actin filaments for targeting by, or protection against, gelsolin-mediated depolymerization.

MATERIALS AND METHODS

Protein purification

Tpm1.12 and Tpm3.1 isoforms were cloned into a pET28a expression plasmid, and Tpm expression in *Escherichia coli* BL21 (DE3) cells, and purification was carried out as described previously (26), with slight modifications. The lysis buffer for the resuspended bacterial pellets additionally contained 10 mM imidazole, 1 mM β-mercaptoethanol, 1% Triton-X 100, and 2 mM $CaCl_2$, and the lysate was centrifuged at 440,000 $\times$ *g* for 1 h at 4°C. The protein concentration was measured using a BCA protein assay kit (Sigma, St. Louis, MO), and the protein preparations were stored at 0°C in 10 mM Tris, 10 mM KCl, and 1 mM dithiothreitol (pH 7.8).

For the preparation of gelsolin, a His-tagged full-length sequence in a pET21d(+) vector was used (27). Plasmid DNA was transformed into *E. coli* BL21 (DE3) cells; a fresh colony was grown in Luria broth at 37°C until OD_{600} = 0.6–0.8 and then induced with 1 mM isopropyl β-D-1-thiogalactopyranoside overnight at 25°C. The cells were collected by centrifugation (Sigma 4-16KS tabletop centrifuge, 6000 $\times$ *g*, 5 min, 4°C), lysed in 5 mM Tris, 300 mM NaCl, 5 mM imidazole, 1 mM ATP, 1 mM phenylmethylsulfonylfluoride, 7 mM β-mercaptoethanol, 30 μg/mL DNase, and protease inhibitor cocktail (P8465, Sigma-Aldrich) (pH 8.0), then sonicated and ultracentrifuged (440,000 $\times$ *g*, 35 min, 4°C; MLA80, Beckman-Coulter, Brea, CA). The supernatant was applied to an Ni-NTA column (Macherey-Nagel, Düren, Germany), washed with lysis buffer, and eluted with 250 mM imidazole in lysis buffer. Fractions containing gelsolin were dialyzed (20 mM Tris and 1 mM EGTA (pH 8.0)) and further purified on a Source 15Q anion exchange column with the application of 50 mL buffer I (20 mM Tris, 20 mM NaCl, and 1 mM EGTA (pH 8.0)), 50 mL buffer II (10 mM Tris and 0.1 mM EGTA (pH 8.0)), 50 mL buffer III (20 mM Tris and 2 mM $CaCl_2$ (pH 8.0)), and a 100 mL linear gradient of buffer III and buffer IV (20 mM Tris, 1 M NaCl, and 0.1 mM EGTA (pH 8.0)). The gelsolin-containing fractions from the last elution step were dialyzed (5 mM HEPES, 50 mM NaCl, and 0.1 mM EGTA (pH 8.0)), loaded on a Superdex 200 gel filtration column equilibrated with dialysis buffer, and eluted. Purified gelsolin was collected, concentrated (4-16KS tabletop centrifuge (Sigma Aldrich) and Vivaspin 10K cut-off tubes (Sartorius, Göttingen, Germany), 3000 $\times$ *g*, 4°C) and stored at −80°C. The protein concentration was measured by spectrophotometry (ε_{280} = 1.29 mL mg^{-1} cm^{-1}).

Actin was prepared from rabbit hind leg muscle (28) and gel filtered on a Superdex G75 (GE Healthcare, Little Chalfont, UK) column in buffer A

(4 mM Tris, 0.2 mM ATP, 0.1 mM $CaCl_2$, 0.5 mM β-mercaptoethanol, and 0.005% NaN_3 (pH 7.8)). G-actin was stored on ice in buffer A. For the fluorescence measurements, actin was labeled with pyrenyl-iodoacetamide as described previously (pyrene; Invitrogen, Carlsbad, CA) (29). Skeletal muscle Tpm (skTM, Tpm1.1) was retrieved from the insoluble residue of the acetone powder from the actin preparation (30), then further purified by hydroxyapatite chromatography and stored frozen in 5 mM Tris and 1 mM dithiothreitol (pH 7.8). The protein concentrations were measured photometrically using $\varepsilon_{280} = 1.11$ mL mg^{-1} cm^{-1} and $\varepsilon_{290} = 0.63$ mL mg^{-1} cm^{-1} extinction coefficients for actin, and $\varepsilon_{280} = 0.3$ mL mg^{-1} cm^{-1} for skTM.

Surface plasmon resonance

The interactions of Tpms with gelsolin were analyzed by surface-Plasmon-resonance (SPR)-based binding technique using the Biacore 3000 instrument (Biacore, GE Healthcare). The Tpm isoforms were directly immobilized onto the sensor chip (CMD500L; XanTec Bioanalytics, Düsseldorf, Germany) via primary amine groups of the proteins using the amine coupling method as recommended by the manufacturer. The surface was first activated by an injection of 35 μL *N*-ethyl-*N*′ (dimethylaminopropyl) carbodiimide/N-hydroxysuccinimide (Biacore, GE Healthcare) solution (200 mM *N*-ethyl-*N*′ (dimethylaminopropyl) carbodiimide and 50 mM N-hydroxysuccinimide); then, the Tpm was diluted to 30 μg/mL in the immobilization buffer (10 mM Na-acetate (pH 3.5)) and injected over the surface for 7 min at a 10 μL/min flow rate. Excess reactive sites were subsequently blocked by injection of 1 M ethanolamine (pH 8.5) (Biacore, GE Healthcare) for 7 min at a flow rate of 5 μL/min. The control surface was activated and then blocked with ethanolamine. After the immobilization of the Tpms, gelsolin was diluted in actin polymerization buffer (4 mM Tris, 0.2 mM ATP, 0.1 mM $CaCl_2$, 0.5 mM β-mercaptoethanol, 0.005% NaN_3, 2 mM $MgCl_2$, and 100 mM KCl (pH 7.8)) and injected over the surfaces at various concentrations (0.5, 1, 2, 3, 4, 5, and 7.5 μM) at a flow rate of 10 μL/min.

The association phases of the interactions between gelsolin and the Tpm were monitored for 7 min and the dissociation phases in polymerization buffer without the gelsolin were monitored for 6 min to determine the kinetic parameters of association and dissociation for the interactions. The sensor chips were regenerated after each binding assay by a brief injection of 10 mM glycine-HCl (pH 2.1). The binding of gelsolin to the immobilized proteins was monitored as a sensorgram where the resonance unit values were plotted against time. The resonance unit measured at the control surface was subtracted from the data obtained for the protein surfaces. Kinetic parameters were evaluated by the BIAevaluation 3.1 software (Biacore, GE Healthcare) assuming a 1:1 gelsolin/Tpm dimer interaction between the proteins.

Fluorescence measurements

Fluorescence experiments were performed with an FLX-Xenius (SAFAS) multichannel spectrofluorimeter. Pyrene fluorescence was excited at 365 nm, and the emission was detected at 407 nm. Polymerization and depolymerization kinetics were followed by measuring the changes of pyrene fluorescence with time at room temperature. The final concentration of $CaCl_2$ was 100 μM, if not indicated otherwise. Actin and other protein components were gently mixed in a 0.6 mL Eppendorf tube immediately before adding them into the cuvettes, which resulted in a few seconds of dead time. Average rates from at least three independent measurements were calculated. Data are given as the mean $\pm$ SE throughout.

Polymerization assays

Ca^{2+}-G-actin labeled with pyrene (5%) was polymerized in buffer A complemented with 2 mM $MgCl_2$ and 100 mM KCl (final concentrations), gelsolin, and different amounts of Tpm. The gelsolin/Tpm complexes were made up in stocks of 0.3 μM gelsolin and 10 μM Tpm for further dilution, and let stand for at least 30 min at room temperature. The progress of actin assembly was monitored by measuring the increase in pyrenyl fluorescence emission. The net rate of actin polymerization was calculated by linear fitting to the segment of the curves between 0.05 and 0.25 normalized fluorescence intensity.

Dilution-induced depolymerization assays

Ca^{2+}-G-actin in buffer A at 10 μM concentration labeled by pyrene (70–80%) was polymerized for 1 h by adding 2 mM $MgCl_2$ and 100 mM KCl (final concentrations); then, Tpms were added and the samples were incubated for 1 h at room temperature. These F-actin samples were then diluted to 100 nM with Ca^{2+}-free polymerization buffer supplemented with 0.1 M $CaCl_2$ to obtain the desired Ca^{2+} concentrations. The gelsolin/Tpm complexes were prepared as described in the previous section and added in the dilution step. Depolymerization rates were estimated by linear fitting to the first 120 s of the normalized pyrene transient curves.

Co-sedimentation assays

The co-sedimentation of gelsolin with actin and Tpms was studied in two complementary experiments. 1) First, 2 μM gelsolin was added to 25 μM F-actin and incubated for 1 h; then, the samples were diluted to 10 μM actin concentration and 0.8 μM gelsolin with different Tpm isoforms (40 μM Tpm1.12, 40 μM Tpm3.1, or 10 μM skTM), with a control sample diluted in polymerization buffer only, and let stand for 2 h. 2) Alternatively, 10 μM F-actin was incubated for 2 h with or without the same concentrations of Tpms as in protocol 1; then, the samples were treated with 0.8 μM gelsolin for 1 h. All measurements were performed using polymerization buffer containing 0.1 mM $CaCl_2$. Samples (100 μL) were pelleted by ultracentrifugation (Beckman-Coulter, TLA-100, 440,000 $\times$ *g* for 30 min at 20°C); then, pellets and supernatants were separated and analyzed by sodium dodecyl sulfate polyacrylamide gel electrophoresis (31). The gels were stained with Coomassie Blue and images were made with ultraviolet illumination (Syngene Bioimaging System, Haryana, India). The protein bands on the gels were quantified using densitometry (software by GeneTools, Philomath, OR). The relative amounts of actin in the pellets were calculated by dividing the actin content of the samples by the actin content of the control sample containing only actin, which was prepared under the same conditions. The relative amounts of gelsolin in the pellets were derived by dividing the gelsolin content of the samples by the gelsolin content of the control sample containing only actin and gelsolin, which was prepared under the same conditions. Data from three independent measurements are given as the mean $\pm$ SE.

Statistical analysis

Statistical significance levels were obtained by two-tailed t-probe in Microsoft Excel. By convention, $p \geq 0.05$ was considered as statistically not significant.

RESULTS AND DISCUSSION

Tpms bind gelsolin

Previous studies indicated that Tpm can bind directly to gelsolin (24,25). We have carried out SPR-based binding experiments to determine the binding affinity of gelsolin for skeletal muscle and non-muscle Tpm isoforms. Tpm isoforms were immobilized by amine coupling on the surface

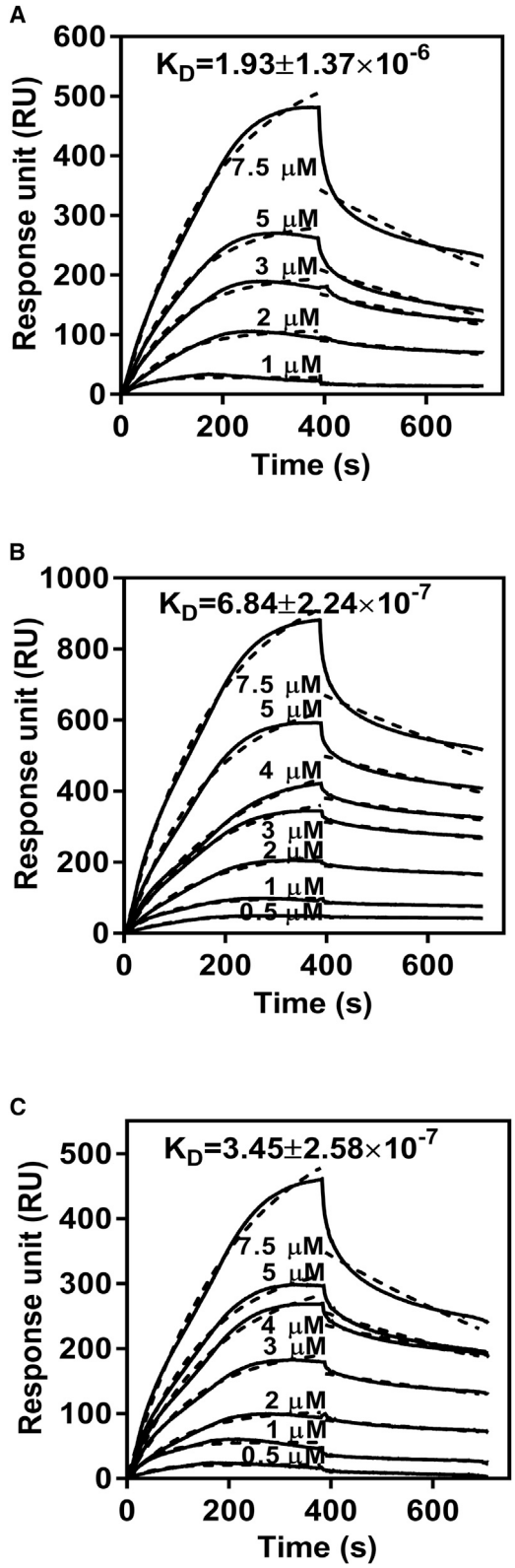

FIGURE 1 Binding of gelsolin to Tpm immobilized on a CMD500L sensor chip at 25°C. The Tpm isoforms were immobilized on the surface of a CMD500L sensor chip by the amine coupling method, and the reference surface was blocked with 1 M ethanolamine solution. The immobilized Tpm isoforms are (*A*) skTM, (*B*) Tpm1.12, and (*C*) Tpm3.1. The interactions between gelsolin and Tpm isoforms were assayed by injecting the gelsolin over the Tpm and reference surfaces at the indicated concentrations for 7 min; then, the dissociation phase was recorded by changing the gelsolin solution to polymerization buffer for 6 min. Kinetic parameters and equilibrium dissociation constants (K_D) for the interactions were derived by the BIAevaluation 3.1 software. Dashed lines indicate the fits for the experimental curves assuming a 1:1 interaction model between the binding partners. The K_D values in molars are indicated on the figures.

of sensor chips, and then gelsolin was run over the surfaces at different concentrations. The SPR sensorgrams obtained in these experiments, including the association (with injected gelsolin) and dissociation (when gelsolin is exchanged for polymerization buffer) phases are presented in Fig. 1. The sensorgrams were fitted with single-exponential functions to determine the corresponding second-order association (k_a) and first-order dissociation rate constants (k_d), and the ratios of these parameters (k_d/k_a) were used to calculate the corresponding dissociation constants (K_Ds) for the interaction of gelsolin with skTM (Fig. 1 *A*: $K_D = 1.9 \pm 1.4$ μM), Tpm1.12 (Fig. 1 *B*; $K_D = 0.7 \pm 0.2$ μM), and Tpm3.1 (Fig. 1 *C*; $K_D = 0.3 \pm 0.2$ μM). These K_D values indicate relatively tight affinities between gelsolin and the Tpms, which fall within the range one would expect for physiologically significant protein-protein interactions, indicating that the binding of gelsolin to Tpms probably has functional consequences.

Gelsolin accelerates actin polymerization in vitro

Next, we tested whether the binding of Tpms to gelsolin affects the corresponding activities of these proteins. Gelsolin is known to accelerate the polymerization of actin through nucleation followed by pointed-end elongation (18). First, we characterized the recombinant gelsolin in a nucleation assay. Polymerization of Ca-actin was carried out in the absence or presence of gelsolin at different concentrations (2–500 nM) (Fig. 2 *A*). Salt-induced actin polymerization is described by the initial slow nucleation step (1–2 min), an ascending elongation phase, and a steady-state phase, where the addition and dissociation of actin monomers are in equilibrium. Addition of nanomolar concentrations of gelsolin increased the initial rate of actin assembly, as reflected by the increasing slope of the curves (Fig. 2, *B* and *C*). The time required for the slow lag phase, corresponding to the nucleation step, became shorter with increasing gelsolin concentrations. This observation was consistent with the known nucleating activity of gelsolin (18).

At higher gelsolin concentrations (>200 nM), the polymerization curves displayed an overshoot, which may be explained by the severing and monomer-sequestering activities of gelsolin. When the proportion of gelsolin relative to actin was low these effects were not dominant, since most of the gelsolin was consumed for nucleation, resulting in capped filaments. Increasing the gelsolin/actin ratio possibly leaves more free gelsolin to sever the elongating filaments,

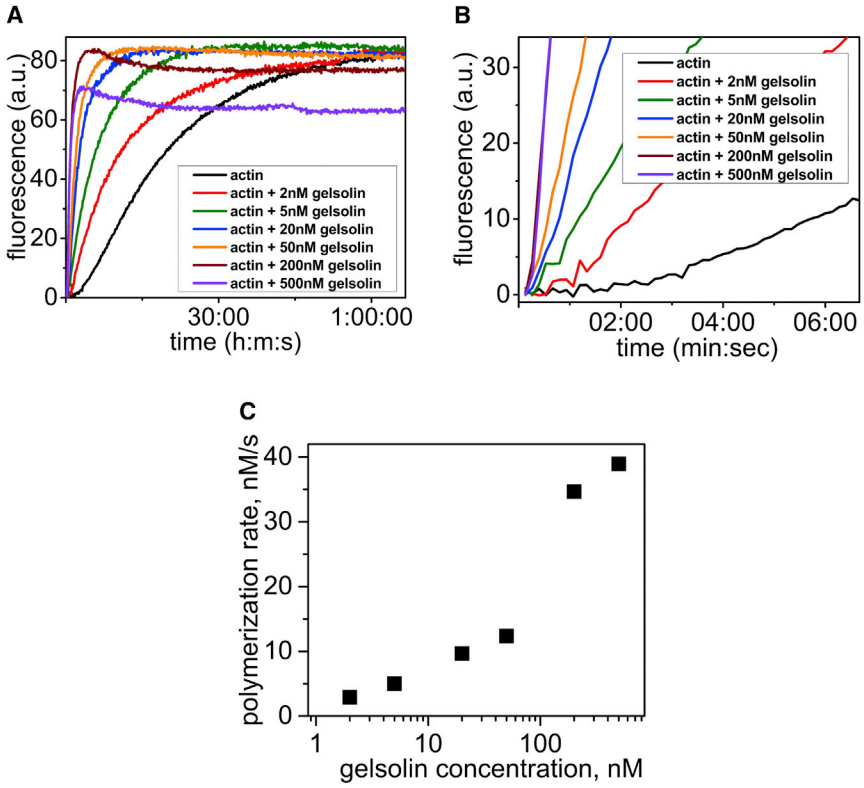

FIGURE 2 Gelsolin increases the rate of actin polymerization. (*A*) Gelsolin was added to 3 μM G-actin at different final concentrations and polymerization was followed by pyrene fluorescence. Data are representative curves from experiments repeated four times. (*B*) The same results as in (*A*) are plotted on a shorter timescale to demonstrate the disappearance of the initial lag phase of nucleation as an effect of gelsolin. (*C*) Representative actin polymerization rates calculated from the slope of the initial 5–25% segment relative to the plateau fluorescence intensity. To see this figure in color, go online.

rendering them shorter. The height of the steady-state plateau phase decreased proportionally to the amount of gelsolin added (Fig. 2 *A*). This likely reflects gelsolin sequestration of actin monomers, preventing their incorporation into filaments and resulting in lower fluorescence intensity. All these observations indicate that the recombinant gelsolin behaves as expected based on previous reports.

Tpms enhance the effect of gelsolin on actin polymerization

Smooth muscle Tpm was reported to inhibit the severing of actin filaments by gelsolin and to have no effect on its actin nucleating activity (25). We investigated whether other Tpm isoforms can influence the effects of gelsolin on actin polymerization. Actin was polymerized in the presence of gelsolin or gelsolin-Tpm complexes. In the latter cases, gelsolin and Tpm were pre-incubated for 30 min in the presence of 100 μM Ca^{2+}. The rate of gelsolin-mediated actin polymerization was increased by all Tpm isoforms (Fig. 3 *A*). To quantify the effects of Tpms, we calculated the elongation rates from the initial 5–25% segments of the transients relative to the maximal fluorescence intensity. The smallest effect on actin assembly was observed with Tpm1.12 (20%; Fig. 3 *B*), a medium effect with Tpm3.1 (57%), and the largest with skTM (76%). The statistical significance level for all three Tpm isoforms was $p < 0.005$. In control experiments, we found that in the absence of gelsolin, Tpms at the applied concentrations did not influence the rate of actin polymerization (Fig. 3 *C*). One possibility for the faster polymerization kinetics is that Tpms may promote the nucleating activity of gelsolin. Another possible mechanism by which Tpms may increase the rate of actin polymerization is to enhance the severing activity of gelsolin that is expected to produce more free filament ends for the monomer association.

Tpms alter the rate of actin filament disassembly catalyzed by gelsolin

To investigate the effect of Tpms on the severing activity of gelsolin, depolymerization measurements were carried out. We used pre-formed pyrene-labeled actin filaments that were subsequently diluted to concentrations below the critical concentration of the barbed end ($\sim$0.12 μM) (32,33). Under these conditions, the incorporation of free actin monomers was negligible, so spontaneous subunit dissociation from the filament ends could be monitored. The spontaneous disassembly kinetics of actin filaments was relatively slow due to the low rate constants for dissociation of actin subunits and also to the low concentration of filament ends (Fig. 4, *left column*, *black lines*). Severing by gelsolin increases the number of pointed ends but caps the barbed ends, resulting in a higher net rate of depolymerization (Fig. 4, *left column*, *green lines*) that was consistent with previous observations (34). When

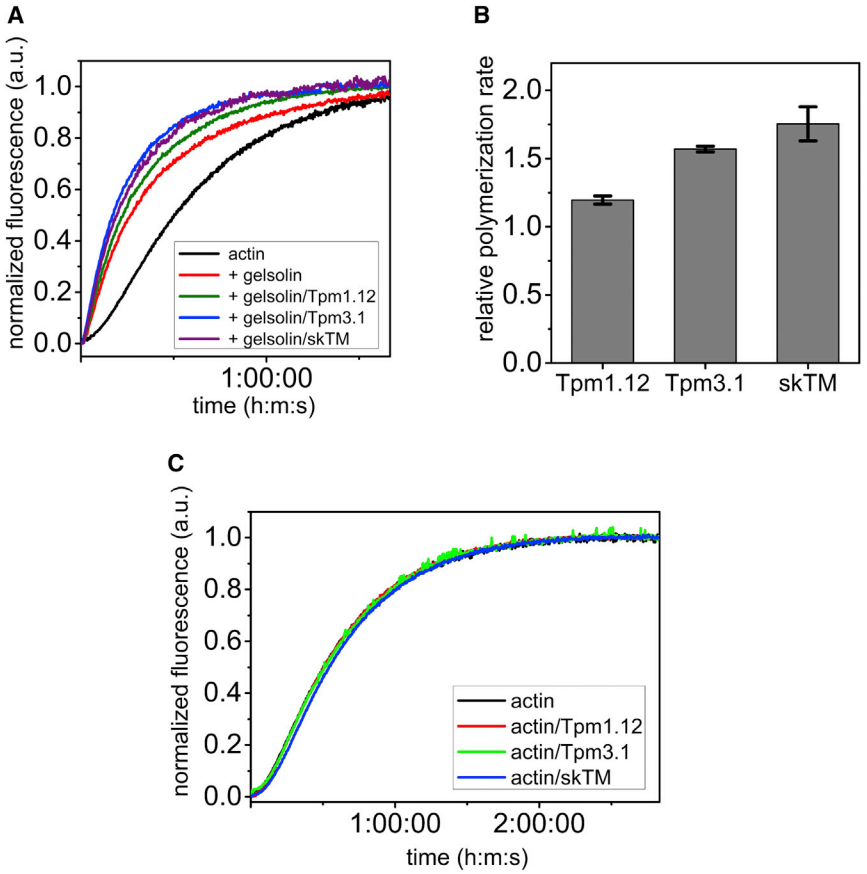

FIGURE 3 Tropomyosins enhance the effect of gelsolin on actin polymerization. (*A*) In these assays, 2 μM actin was polymerized alone or in the presence of either 4.5 nM gelsolin or 4.5 nM gelsolin preincubated with different Tpm isoforms. Gelsolin and Tpms were prepared in stock solutions for 30 min after mixing them at 300 nM and 10 μM concentrations, respectively. (*B*) The enhancement of the polymerization rate with Tpm-complexed gelsolin over gelsolin alone was calculated from the slope of the 5–25% segment of the pyrenyl traces relative to the plateau fluorescence intensity ($n = 6$; data are represented as the mean $\pm$ SE). The statistical significance level for all three Tpm isoforms was $p < 0.005$. (*C*) Polymerization curves for the same amount of actin as in (*A*) with and without Tpms and without gelsolin. To see this figure in color, go online.

pre-incubated gelsolin-Tpm complexes were added to the actin filaments, the rate of decrease in fluorescence was more pronounced than that observed with gelsolin alone, for all three isoforms of Tpm, suggesting higher rates of depolymerization (Fig. 4, *left column*, *green* and *blue lines*, and *middle column*). When Tpms were added to the actin filaments at saturating concentrations in the absence of gelsolin, they did not result in an enhancement of the spontaneous depolymerization rate (Fig. 4, *left column*, *black* and *red lines*, and *middle column*). Moreover, Tpm1.12 and Tpm3.1 slightly inhibited this process, whereas skTM had a much stronger protective effect. These observations are in correlation with our previous results showing that Tpms decrease the rate of the spontaneous depolymerization of Mg^{2+}-F-actin (26). Taken together, these observations lead us to conclude that gelsolin in complex with Tpm has a higher activity for severing actin filaments than gelsolin alone.

The addition of gelsolin to actin filaments saturated with Tpm1.12 or Tpm3.1 had little influence on the rate of depolymerization (Fig. 4, *left column*, *black* and *cyan lines*, and *middle column*). In contrast, skTM seemed to completely prevent the gelsolin effect, resulting in low dissociation rates that were similar to those observed with actin alone. When gelsolin that had been pre-incubated with Tpm was added to actin filaments previously saturated by Tpm, every isoform increased the depolymerization rate as compared to that measured with free gelsolin on Tpm-bound actin filaments (Fig. 4, *left column*, *cyan* and *magenta lines*, and *middle column*). However, in the case of skTM-decorated actin filaments, the depolymerizing effect of gelsolin, either free or bound by Tpm, significantly lagged behind what was obtained for Tpm-free filaments (to approximately the same extent with gelsolin and gelsolin/skTM; ~4- and 3.6-fold, respectively). Since this was not the case for the non-muscle Tpm isoforms, it suggests that the presence of Tpms may differentially influence the fate of the actin filaments related to the gelsolin-mediated depolymerization.

One may also speculate that the final Tpm concentration in the samples was below the level that can keep Tpm in complex with actin and/or gelsolin and their dissociation had resulted in the different abilities to protect filaments from depolymerization. In this respect, skeletal Tpm required the lowest concentration to saturate F-actin, but in contrast gave the highest protective effect. Therefore, we carried out depolymerization experiments also by diluting samples into buffers containing additional Tpm (data not shown). The final Tpm concentrations were calculated considering the dissociation constants and were kept above the saturation levels of both actin filaments and gelsolin (5 μM skTM, 5 μM Tpm1.12, and 3 μM Tpm 3.1). We

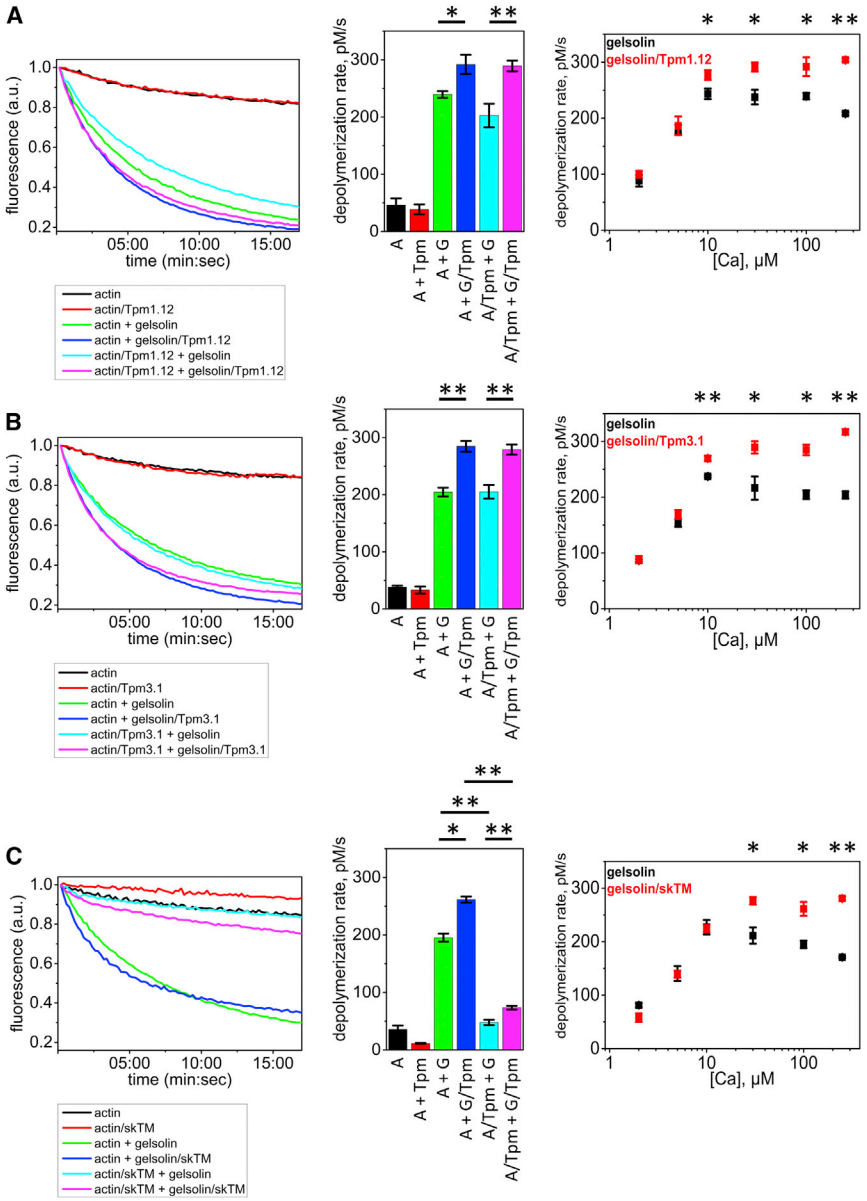

FIGURE 4 Tropomyosins enhance the actin-filament severing activity of gelsolin. For the depolymerization assays, 3 μM actin was polymerized alone or in the presence of 30 μM Tpm1.12, 30 μM Tpm3.1, or 10 μM skTM. The samples were diluted into polymerization buffer to a final concentration of 100 nM to induce spontaneous depolymerization. Gelsolin (300 nM) was prepared with or without 10 μM Tpm and was added to a 4 nM final concentration concomitant with the dilution of F-actin. Results are shown for Tpm1.12 (*A*), Tpm3.1 (*B*), and skTM (*C*). In these experiments, buffers for dilution were prepared from calcium-free polymerization buffer supplemented with 0.1 M $CaCl_2$ to the desired concentration. In the left column, representative depolymerization curves of parallel measurements are plotted. In the middle column, net depolymerization rates are shown calculated from the initial nearly linear 2-min parts of the dissociation curves. (The color scheme is *black*, actin; *red*, actin/Tpm; *green*, actin + gelsolin; *blue*, actin + gelsolin/Tpm; *cyan*, actin/Tpm + gelsolin; *magenta*, actin/Tpm + gelsolin/Tpm.) In the right column, dependence of the depolymerization rate on calcium concentration is plotted for gelsolin alone or gelsolin/Tpm complexes added to F-actin upon dilution. Data are given as the mean ± SE; n = 4–6. *$p < 0.05$; **$p < 0.01$. To see this figure in color, go online.

found that the results with or without additional Tpm differed by a statistical significance level of $p < 0.05$ only in two cases, first when F-actin was mixed with the gelsolin/skTM complex, and second when gelsolin was added to the actin/Tpm3.1 complex. In all other cases, any increase in protection was statistically not significant. These observations suggest that individual Tpm isoforms bound to actin filaments do have different abilities to inhibit the severing activity of gelsolin. Furthermore, the data indicate that on the timescale of the depolymerization rate measurements the dissociation of the Tpm complexes with actin or gelsolin is negligible.

To study the effect of calcium concentration on the severing activity of gelsolin, we completed a series of experiments varying the free calcium concentrations. The disassembly of actin filaments was dependent on the calcium concentration both with gelsolin alone and with gelsolin in complex with Tpm. The depolymerization rate increased up to 10 μM Ca^{2+} in both cases, and above this concentration, the rates showed saturation (Fig. 4, *right column*). The Tpms showed no effect at the lowest calcium ion concentration (2 μM), indicating that they do not activate gelsolin. In the low-calcium ascending phase the effect of gelsolin alone was not different from that of the gelsolin/Tpm complexes, but in the saturating calcium region, the latter had a higher depolymerization rate than gelsolin alone at all Ca^{2+} concentrations tested. At the highest calcium concentrations (100 and 250 μM), the activity of gelsolin declined slightly again, but the gelsolin/Tpm complexes did not show a similar tendency.

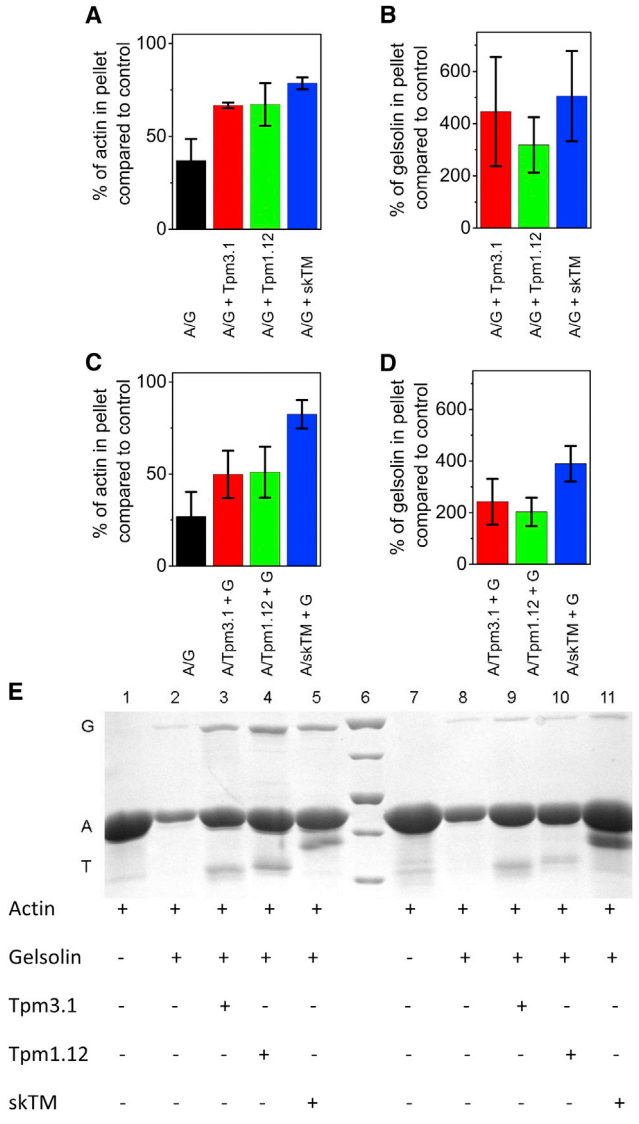

FIGURE 5 Tropomyosins differently protect actin filaments from depolymerization by gelsolin. (*A* and *B*) In the co-sedimentation study, 25 μM F-actin was treated with 2 μM gelsolin for 1 h, then diluted to 10 μM (gelsolin to 0.8 μM) in the presence of either 40 μM Tpm1.12, 40 μM Tpm3.1, or 10 μM skTM. The samples were incubated for 2 h, then ultracentrifuged, and the pellets were analyzed by densitometry. Controls containing only actin filaments and complexes of actin with gelsolin were also prepared. (*A*) Bars represent the relative sedimented actin content compared with F-actin alone (The color scheme is *black*, actin/gelsolin; *red*, actin/gelsolin + Tpm3.1; *green*, actin/gelsolin + Tpm1.12; *blue*, actin/gelsolin + skTM). (*B*) Bars indicate the relative gelsolin content compared with the actin/gelsolin sample (colors are the same as for *A*). (*C* and *D*) In the reverse experiment, first, 10 μM F-actin was prepared for 2 h alone or with 40 μM Tpm1.12, 40 μM Tpm3.1, or 10 μM skTM, and then, 0.8 μM gelsolin was added for 1 h. Bars and colors are the same as in (*A*) and (*B*). Data are given as the mean $\pm$ SE; n = 3. (*E*) Sodium dodecyl sulfate polyacrylamide gel electrophoresis of the co-sedimentation samples representing the changes in the protein contents. Samples 1–5 were subjected to experimental setup 1 (for *A* and *B*) and samples 7–11 to experimental setup 2 (for *C* and *D*). Samples 1 and 7 were actin, samples 2 and 8 were actin + gelsolin, sample 3 was actin/gelsolin + Tpm3.1, sample 4 was actin/gelsolin + Tpm1.12, sample 5 was actin/gelsolin + skTM, column 6 is a molecular weight marker (bands from the top to bottom are 100, 70, 50, 40, and 30 kDa), sample 9 was actin/Tpm3.1 + gelsolin, sample 10 was actin/Tpm1.12 + gelsolin, and sample 11 was actin/skTM + gelsolin. Proteins on the gel are marked as G (gelsolin), A (actin), or T (Tpms). To see this figure in color, go online.

Tropomyosins protect actin filaments from gelsolin in co-sedimentation experiment

To further describe the interactions between actin, gelsolin, and Tpm we carried out co-sedimentation experiments. The samples containing these three proteins were centrifuged and the pellets and supernatants were analyzed using sodium dodecyl sulfate polyacrylamide-gel electrophoresis. Two experimental strategies were applied. First, actin filaments were incubated with gelsolin to provide enough time for their depolymerization, and then Tpm was added to the samples. In the second set of experiments, actin was incubated with Tpm to allow equilibrium for filament complex formation and gelsolin was added afterward.

When gelsolin (0.8 μM) was added to 10 μM F-actin, it reduced the pelleted actin to ~35–40% (Fig. 5 *A*). When Tpm was subsequently added to the samples, the amount of actin in the pellets increased, suggesting that the Tpm isoforms partially rescued the actin filaments from the severing effect of gelsolin. The possibility that the accumulation of pelleted actin resulted from de novo filament assembly driven by Tpms was not considered, since Tpms do not promote this process (26). When the gelsolin content in the pellets of the Tpm-treated samples was compared with the samples containing only actin and gelsolin, there was a two- to fivefold increase in gelsolin in all cases (Fig. 5 *B*). In control experiments, Tpms without actin did not influence the sedimentation of gelsolin (data not shown).

When Tpm was added to the actin filaments before the administration of gelsolin, a two- to threefold increase in the amount of pelleted F-actin was observed compared to that in the absence of Tpm (Fig. 5 *C*). This suggests that Tpms have also a prior protective effect against the severing activity of gelsolin. These results are consistent with our observations in the fluorescence spectroscopy measurements (Fig. 4). The amount of gelsolin sedimented was again two- to fourfold higher with actin and Tpm than with actin alone. The relative increment of the gelsolin content in the Tpm-treated samples exceeded that of the F-actin alone when the first strategy was applied but was not significant with the second (Fig. 5 *D*). This suggests that gelsolin is not able to bind to Tpm molecules decorating actin filaments. In contrast, it seems possible for gelsolin bound to Tpm to incorporate into existing actin filaments (see previous section).

CONCLUSIONS

Previous studies extended the experimental evidence for the importance of Tpm isoforms in specifying the functional

properties of actin filaments (5,7). According to those studies, Tpm function relies on the ability of Tpm isoforms to affect the interaction of ABPs with actin filaments, which is manifested through steric- or allosteric-mechanism-based competitive binding of Tpm isoforms and ABPs, such as Arp2/3 complex (26,32,35,36), ADF/cofilins (37), α-actinin (3), and myosins (3). In this work, we extended the investigations of the Tpm isoform specificity of actin interactions by addressing the binding of gelsolin and Tpms and its functional consequences in actin dynamics regulation.

We found that Tpm could potentially protect the actin filaments from the depolymerizing/severing activity of gelsolin. This effect showed strong dependence on the bound Tpm isoform. The skeletal muscle Tpm1.1/1.2 isoform was the most efficient, whereas the two non-muscle short isoforms—Tpm3.1 and Tpm1.12—had little or no significant influence on the depolymerizing activity of gelsolin. Considering that the overall structure of the Tpm-actin copolymer is isoform specific (38), we propose that some Tpm isoforms can structurally interfere with the binding of gelsolin to actin, whereas others have no competitive effect on the actin binding of gelsolin. Examples for such cases are provided in Fig. 6. In the cell, the position of the various Tpms on the actin-filament surface will likely be further modulated by the interaction of Tpms with other ABPs.

We demonstrated that all three Tpm isoforms bind to gelsolin and that their interactions are characterized by similar and relatively tight affinities ($K_D \sim 0.3$–2.0 μM). From this aspect, gelsolin binding to Tpm has only little specificity for Tpm isoforms, which suggests that the binding interactions rely on a common Tpm sequence pattern. As a functional consequence, we showed that gelsolin is more efficient in disassembling actin filaments when it is in complex with Tpm than in its free form, even if the actin filaments are saturated by Tpms. The low concentrations of actin and Tpm in the depolymerization tests restrict their binding to a negligible level, so the observed effects of enhanced gelsolin activity can only be explained as a direct impact of Tpm on the gelsolin in their complex. We could exclude the mechanism where Tpm first binds gelsolin and then serves only to deliver gelsolin to the sides of actin filaments. These findings suggest that the binding of Tpm induces structural changes in gelsolin, which modify its interaction mode and activity with actin filaments. The increase in the rate of depolymerization observed for the gelsolin-Tpm complexes can be explained by the enhanced filament cutting efficiency of gelsolin and/or the weakened filament-end interactions proposed in a previous study (23). Our findings are seemingly in contrast to formerly reported observations where muscle Tpm isoforms decreased the gelsolin-catalyzed depolymerization rate of actin filaments (25). Also, we have opposite results with the Tpm-decorated actin filaments where a protective effect was observed against the gelsolin activity. These discrepancies are not easy to interpret. Our results showing that saturation of F-actin with Tpm inhibits gelsolin activity were uniform in our depolymerization assays and bulk co-sedimentation tests, and are in accordance with literature data (22).

Both studies used the pyrenyl-actin-based dilution-induced disassembly assay, but a marked difference has to be noted. In our experiments, actin filaments were diluted to 100 nM, which is a true depolymerizing regime; therefore, the change in pyrene fluorescence reflects only disassembly. In contrast, Kaithlina et al. (33) used 600 nM gelsolin-capped actin filaments, which is around the critical

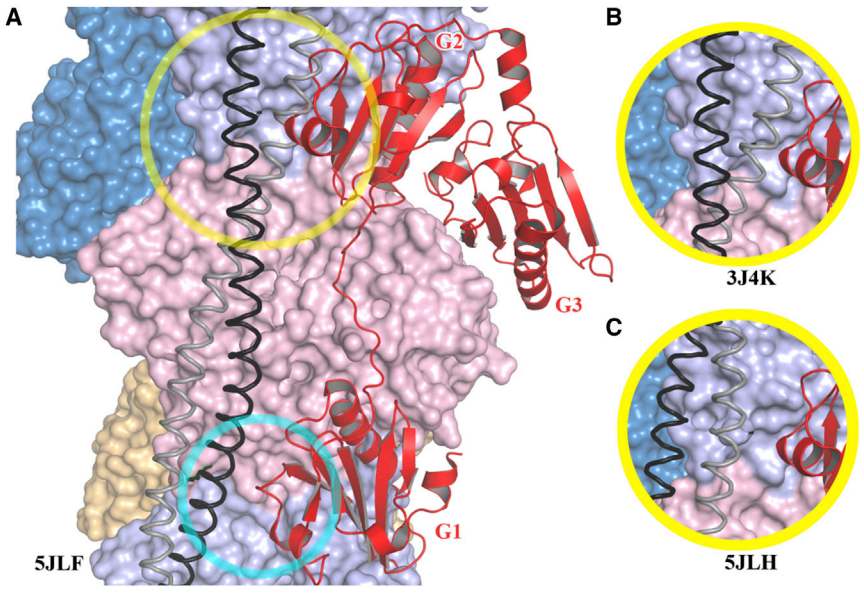

FIGURE 6 Models of Tpm (*gray* and *black coils*) and gelsolin G1–G3 (*red ribbons*) binding to an actin filament (subunits represented as surfaces in pastel shades). (*A*) Gelsolin domains from the G1–G3/actin x-ray structure (PDB: 3FFK) (27) docked onto the cryo-EM structure of 3.5 Å mouse skTM/actin (PDB: 5JLF) (42) through superimposition of an actin protomer structure (*pink*). In this model, G1 does not sterically clash with Tpm (*cyan circle*), but G2 has significant overlap (*yellow circle*). (*B* and *C*) Close-ups of the Tpm/G2 interaction (*yellow circle*) generated from the 8 Å cryo-EM structure of chicken gizzard Tpm/actin (PDB: 3J4K) (43) (*B*) and from the cryo-EM structure of 3.9 Å human cytoplasmic Tpm3/actin/myosin (PDB: code 5JLH) (42) (*C*). These models are not intended to be accurate representations of a gelsolin/actin/Tpm interaction, but rather to indicate that the known position of Tpms on actin are in locations that could have a variety of competitive effects on gelsolin binding. Thus, the positional placement of Tpms on the surface of the actin filament will dictate whether gelsolin can simultaneously bind to the same actin filament. To see this figure in color, go online.

concentration of pointed ends but well above the critical concentration of barbed ends; therefore, the changes in pyrene fluorescence could be distorted by assembly events.

Our results are in accordance with the general assumption about the functional significance of the Tpm diversity. It is proposed that Tpms work as key regulators of the microfilament system (39) to specify spatially and functionally individual actin subsets, with distinct regulation of the interactions with other ABPs. The Tpm isoform composition of the actin filaments would be, then, a principal factor that defines the location, supramolecular organization, and role of actin filaments in cellular physiology. On the other hand, other ABPs also can specify which Tpm isoforms bind to the growing actin filaments, as shown for formin proteins (40).

In terms of the emergence of gelsolin and Tpm in evolution (14,41), current evidence suggests that gelsolins are the more ancient actin regulators. Thus, the later appearance of Tpms seems to allow specification of populations of actin filaments, which with respect to gelsolin have different activities. In particular, our data suggest that muscle actin structures will be stabilized relative to general cytoplasmic actin filaments in muscle cells.

Taken together, our work demonstrates that the studied Tpms have dual effects on the actin-assembly-promoting activity of gelsolin. When Tpms are in complex with actin filaments, they inhibit depolymerization by gelsolin in an isoform-dependent manner. In contrast, when Tpms are bound to gelsolin they enhance this activity in an isoform-independent fashion. These observations provide an important contribution toward understanding the necessity and different functions of the large number of Tpm isoforms located and active in living cells. It requires further studies to demonstrate whether gelsolin-Tpm complexes play a physiological role in the regulation of actin dynamics in living cells and how the calcium concentrations applied in this work are relevant in vivo.

ACKNOWLEDGMENTS

We express our special thanks to Ilona Brunner and Éva Simon for their technical skills and essential contributions to the protein preparation. This scientific contribution is dedicated to the 650th anniversary of the foundation of the University of Pécs, Hungary.

This work was supported by grants from the National Research, Development and Innovation Office and the European Union (GINOP-2.3.3-15-2016-00025, GINOP-2.3.2-15-2016-00049, and EFOP-3.6.1-16-2016-00004) and by the Hungarian Science Foundation (OTKA grants K112794 to M.N., K109689 to B.B., and K109249 to F.E.). This research was supported in addition by the European Union and the State of Hungary, co-financed by the European Social Fund in the framework of TÁMOP 4.2.4.A/2-11-1-2012-0001 "National Excellence Program" and the New National Excellence Program of the Ministry of Human Capacities (to B.B. and T.H.), and by the ÚNKP-16-4 and ÚNKP-17-4 New National Excellence Program of the Ministry of Human Capacities (to B.B.). R.C.R. was supported by the Biomedical Research Council, Agency for Science, Technology and Research (A*STAR), Singapore.

REFERENCES

1. Perrin, B. J., and J. M. Ervasti. 2010. The actin gene family: function follows isoform. *Cytoskeleton (Hoboken).* 67:630–634.
2. Vindin, H., and P. Gunning. 2013. Cytoskeletal tropomyosins: choreographers of actin filament functional diversity. *J. Muscle Res. Cell Motil.* 34:261–274.
3. Gateva, G., E. Kremneva, …, P. Lappalainen. 2017. Tropomyosin isoforms specify functionally distinct actin filament populations in vitro. *Curr. Biol.* 27:705–713.
4. Cooley, B. C., and G. Bergtrom. 2001. Multiple combinations of alternatively spliced exons in rat tropomyosin-α gene mRNA: evidence for 20 new isoforms in adult tissues and cultured cells. *Arch. Biochem. Biophys.* 390:71–77.
5. Gunning, P. W., G. Schevzov, …, E. C. Hardeman. 2005. Tropomyosin isoforms: dividing rods for actin cytoskeleton function. *Trends Cell Biol.* 15:333–341.
6. Flicker, P. F., G. N. Phillips, Jr., and C. Cohen. 1982. Troponin and its interactions with tropomyosin. An electron microscope study. *J. Mol. Biol.* 162:495–501.
7. Gunning, P., G. O'Neill, and E. Hardeman. 2008. Tropomyosin-based regulation of the actin cytoskeleton in time and space. *Physiol. Rev.* 88:1–35.
8. Weinberger, R., G. Schevzov, …, P. Gunning. 1996. The molecular composition of neuronal microfilaments is spatially and temporally regulated. *J. Neurosci.* 16:238–252.
9. Hannan, A. J., G. Schevzov, …, R. P. Weinberger. 1995. Intracellular localization of tropomyosin mRNA and protein is associated with development of neuronal polarity. *Mol. Cell. Neurosci.* 6:397–412.
10. Schevzov, G., P. Gunning, …, R. P. Weinberger. 1997. Tropomyosin localization reveals distinct populations of microfilaments in neurites and growth cones. *Mol. Cell. Neurosci.* 8:439–454.
11. Schevzov, G., B. Vrhovski, …, P. W. Gunning. 2005. Tissue-specific tropomyosin isoform composition. *J. Histochem. Cytochem.* 53: 557–570.
12. Bryce, N. S., G. Schevzov, …, R. P. Weinberger. 2003. Specification of actin filament function and molecular composition by tropomyosin isoforms. *Mol. Biol. Cell.* 14:1002–1016.
13. Nag, S., M. Larsson, …, L. D. Burtnick. 2013. Gelsolin: the tail of a molecular gymnast. *Cytoskeleton (Hoboken).* 70:360–384.
14. Ghoshdastider, U., D. Popp, …, R. C. Robinson. 2013. The expanding superfamily of gelsolin homology domain proteins. *Cytoskeleton (Hoboken).* 70:775–795.
15. Yin, H. L., and T. P. Stossel. 1979. Control of cytoplasmic actin gel-sol transformation by gelsolin, a calcium-dependent regulatory protein. *Nature.* 281:583–586.
16. Finidori, J., E. Friederich, …, D. Louvard. 1992. In vivo analysis of functional domains from villin and gelsolin. *J. Cell Biol.* 116: 1145–1155.
17. Harris, H. E., and A. G. Weeds. 1984. Plasma gelsolin caps and severs actin filaments. *FEBS Lett.* 177:184–188.
18. Yin, H. L., J. H. Hartwig, …, T. P. Stossel. 1981. Ca^{2+} control of actin filament length. Effects of macrophage gelsolin on actin polymerization. *J. Biol. Chem.* 256:9693–9697.
19. Burtnick, L. D., E. K. Koepf, …, R. C. Robinson. 1997. The crystal structure of plasma gelsolin: implications for actin severing, capping, and nucleation. *Cell.* 90:661–670.
20. Robinson, R. C., M. Mejillano, …, S. Choe. 1999. Domain movement in gelsolin: a calcium-activated switch. *Science.* 286:1939–1942.
21. McLaughlin, P. J., J. T. Gooch, …, A. G. Weeds. 1993. Structure of gelsolin segment 1-actin complex and the mechanism of filament severing. *Nature.* 364:685–692.
22. Ishikawa, R., S. Yamashiro, and F. Matsumura. 1989. Differential modulation of actin-severing activity of gelsolin by multiple isoforms of cultured rat cell tropomyosin. Potentiation of protective ability

of tropomyosins by 83-kDa nonmuscle caldesmon. *J. Biol. Chem.* 264:7490–7497.

23. Nyakern-Meazza, M., K. Narayan, …, U. Lindberg. 2002. Tropomyosin and gelsolin cooperate in controlling the microfilament system. *J. Biol. Chem.* 277:28774–28779.
24. Koepf, E. K., and L. D. Burtnick. 1992. Interaction of plasma gelsolin with tropomyosin. *FEBS Lett.* 309:56–58.
25. Khaitlina, S., H. Fitz, and H. Hinssen. 2013. The interaction of gelsolin with tropomyosin modulates actin dynamics. *FEBS J.* 280:4600–4611.
26. Kis-Bicskei, N., A. Vig, …, G. C. Talián. 2013. Purification of tropomyosin Br-3 and 5NM1 and characterization of their interactions with actin. *Cytoskeleton (Hoboken).* 70:755–765.
27. Nag, S., Q. Ma, …, R. C. Robinson. 2009. Ca^{2+} binding by domain 2 plays a critical role in the activation and stabilization of gelsolin. *Proc. Natl. Acad. Sci. USA.* 106:13713–13718.
28. Spudich, J. A., and S. Watt. 1971. The regulation of rabbit skeletal muscle contraction. I. Biochemical studies of the interaction of the tropomyosin-troponin complex with actin and the proteolytic fragments of myosin. *J. Biol. Chem.* 246:4866–4871.
29. Kouyama, T., and K. Mihashi. 1981. Fluorimetry study of N-(1-pyrenyl)iodoacetamide-labelled F-actin. Local structural change of actin protomer both on polymerization and on binding of heavy meromyosin. *Eur. J. Biochem.* 114:33–38.
30. Smillie, L. B. 1982. Preparation and identification of alpha- and β-tropomyosins. *Methods Enzymol.* 85:234–241.
31. Laemmli, U. K. 1970. Cleavage of structural proteins during the assembly of the head of bacteriophage T4. *Nature.* 227:680–685.
32. Bugyi, B., and M. F. Carlier. 2010. Control of actin filament treadmilling in cell motility. *Annu. Rev. Biophys.* 39:449–470.
33. Pollard, T. D. 2007. Regulation of actin filament assembly by Arp2/3 complex and formins. *Annu. Rev. Biophys. Biomol. Struct.* 36:451–477.
34. Tóth, M. A., A. K. Majoros, …, B. Bugyi. 2016. Biochemical activities of the wiskott-aldrich syndrome homology region 2 domains of sarcomere length short (SALS) protein. *J. Biol. Chem.* 291:667–680.
35. Hsiao, J. Y., L. M. Goins, …, R. D. Mullins. 2015. Arp2/3 complex and cofilin modulate binding of tropomyosin to branched actin networks. *Curr. Biol.* 25:1573–1582.
36. Blanchoin, L., T. D. Pollard, and S. E. Hitchcock-DeGregori. 2001. Inhibition of the Arp2/3 complex-nucleated actin polymerization and branch formation by tropomyosin. *Curr. Biol.* 11:1300–1304.
37. Robaszkiewicz, K., Z. Ostrowska, …, J. Moraczewska. 2016. Tropomyosin isoforms differentially modulate the regulation of actin filament polymerization and depolymerization by cofilins. *FEBS J.* 283:723–737.
38. Lehman, W., V. Hatch, …, R. Craig. 2000. Tropomyosin and actin isoforms modulate the localization of tropomyosin strands on actin filaments. *J. Mol. Biol.* 302:593–606.
39. Gunning, P. W., E. C. Hardeman, …, D. P. Mulvihill. 2015. Tropomyosin—master regulator of actin filament function in the cytoskeleton. *J. Cell Sci.* 128:2965–2974.
40. Johnson, M., D. A. East, and D. P. Mulvihill. 2014. Formins determine the functional properties of actin filaments in yeast. *Curr. Biol.* 24:1525–1530.
41. Gunning, P. W., U. Ghoshdastider, …, R. C. Robinson. 2015. The evolution of compositionally and functionally distinct actin filaments. *J. Cell Sci.* 128:2009–2019.
42. von der Ecken, J., S. M. Heissler, …, S. Raunser. 2016. Cryo-EM structure of a human cytoplasmic actomyosin complex at near-atomic resolution. *Nature.* 534:724–728.
43. Sousa, D. R., S. M. Stagg, and M. E. Stroupe. 2013. Cryo-EM structures of the actin:tropomyosin filament reveal the mechanism for the transition from C- to M-state. *J. Mol. Biol.* 425:4544–4555.